CHAPTER TWENTY-ONE

Ultrasound and Magnetic Resonance Microimaging of Mouse Development

Brian J. Nieman[*,†] *and* Daniel H. Turnbull[‡,§]

Contents

Abstract

Ultrasound biomicroscopy (UBM) and magnetic resonance microimaging (micro-MRI) provide noninvasive, high-resolution images in mouse embryos and neonates, enabling volumetric and functional analyses of phenotypes, including longitudinal imaging of individual mice over critical stages of *in utero* and early-postnatal development. In this chapter, we describe the underlying principles of UBM and micro-MRI, including the advantages and limitations of these approaches for studies of mouse development, and providing a number of examples to illustrate their use. To date, most imaging studies have focused on the developing nervous and cardiovascular systems, which are also reflected in the examples shown in this chapter, but we also discuss the future application of these methods to other organ systems.

* Mouse Imaging Centre, Hospital for Sick Children, Toronto, Canada
† Department of Medical Biophysics, University of Toronto, Toronto, Canada
‡ Kimmel Center for Biology and Medicine at the Skirball Institute of Biomolecular Medicine, New York University School of Medicine, New York, USA
§ Departments of Radiology and Pathology, New York University School of Medicine, New York, USA

Methods in Enzymology, Volume 476
ISSN 0076-6879, DOI: 10.1016/S0076-6879(10)76021-3

1. Introduction

Compared to developmental biology studies in lower organisms, such as *Caenorhabditis elegans* and zebrafish, the mouse presents significant challenges for direct visualization and analysis of volumetric and dynamic changes in embryos and their developing organ systems. Despite advances in optical microscopy and the availability of mouse reporter lines expressing fluorescent proteins, *in vivo* optical imaging is generally restricted to tissue explants and *exo utero* imaging of early-stage embryos that are amenable to whole embryo culture, and imaging studies cover relatively short time windows over which normal development can be maintained. Ultrasound and magnetic resonance imaging (MRI) are widely used for human fetal and pediatric imaging, and can be scaled to provide effective microimaging tools for application in mice. Although the spatial resolution of these methods (typically 50–100 μm) is lower than optical microscopy, they offer the advantages of much greater penetration, enabling whole body imaging, and the ability to perform three-dimensional (3D) anatomical and functional phenotype analyses, including noninvasive longitudinal imaging over periods of days to weeks, both *in utero* in mouse embryos, and extending to neonatal through adult stages of organ development. A major challenge for imaging methods, including ultrasound and MRI, is the need for high image throughput necessary to match the requirements for efficient phenotypic screening of mutant and transgenic embryos and postnatal mice. In this context, both ultrasound and MRI offer significant advantages in terms of real-time imaging capability (ultrasound) and the recent development of multiple-mouse imaging systems (MRI). For phenotype screening with either method, the image analysis process is critically important, but is not discussed in detail in this chapter. It is worth noting that MRI data are particularly well-suited to computational 3D analysis approaches, providing the potential to greatly improve phenotyping throughput and detection of more subtle changes than can be evaluated by simple inspection of images. Such methods have produced impressive results in the adult mouse brain (Lerch *et al.*, 2008; Nieman *et al.*, 2006), but have not been employed extensively to date for analysis during development or in other tissues. In principle, however, these and emerging methods can be extended to provide embryonic and neonatal phenotype analysis. Development of such automated phenotyping methods are likely to continue, particularly in the context of embryo imaging, as large-scale efforts to generate mutants of every gene motivate improved high-throughput phenotyping methods. It should also be noted that ultrasound and MRI are two technologies among others that provide similar, often complementary information. Alternative techniques not described here include X-ray computed tomography after

iodine staining or perfusion of X-ray opaque vascular agents (Marxen *et al.*, 2004; Metscher, 2009) and optical projection tomography, which advantageously may also permit the use of immunohistochemical fluorescent markers (Sharpe *et al.*, 2002; Walls *et al.*, 2008). Ultrasound and MRI are notable for their ability to provide *in vivo* data in mouse embryos.

With the recent increase in multimodality small-animal imaging facilities in many research centers, the ability to utilize ultrasound and MRI microimaging is now a reality for many mouse developmental biologists. In this chapter, we describe a variety of ultrasound and MRI methods that are now available for studies of mouse development.

2. Ultrasound Biomicroscopy

Ultrasound is the most common approach for fetal imaging in the clinic. Likewise, ultrasound biomicroscopy (UBM) is now a well-established method for *in utero* imaging of mouse embryos (Srinivasan *et al.*, 1998; Turnbull *et al.*, 1995; reviewed in Turnbull and Foster, 2002). UBM is a high-frequency (30–100 MHz) form of pulse-echo imaging, providing high-resolution (30–100 μm) images in real time. High-frequency Doppler ultrasound has also been incorporated into UBM scanners to measure blood velocity, originally using separate transducers for imaging and Doppler (Fig. 21.1) (Aristizabal *et al.*, 1998), and more recently with both functions provided by the same transducer in commercial scanners (Foster *et al.*, 2009; Zhou *et al.*, 2002). Originally, UBM systems were based on single, mechanically scanned transducers, but more recently array transducers have been developed to improve focusing (Aristizabal *et al.*, 2006) and increase image frame rates using electronic beam forming without the need for mechanical scanning (Foster *et al.*, 2009). *In utero* UBM of mouse embryos is most commonly performed at frequencies between 40 and 50 MHz, which allows sufficient penetration to image mouse embryos throughout gestation with high spatial resolution, starting from early postimplantation stages (Zhou *et al.*, 2002).

2.1. UBM of mouse embryos and neonates

Since its introduction for *in utero* mouse embryo imaging over 15 years ago, UBM has found numerous applications, mostly for brain and cardiovascular imaging (reviewed in Turnbull and Foster, 2002). Similar to clinical ultrasound, Doppler approaches have enabled analysis of blood flow properties in the embryo that provide new insights into development of cardiovascular function (reviewed in Phoon and Turnbull, 2003). The general approach taken for *in utero* UBM studies is to anesthetize the

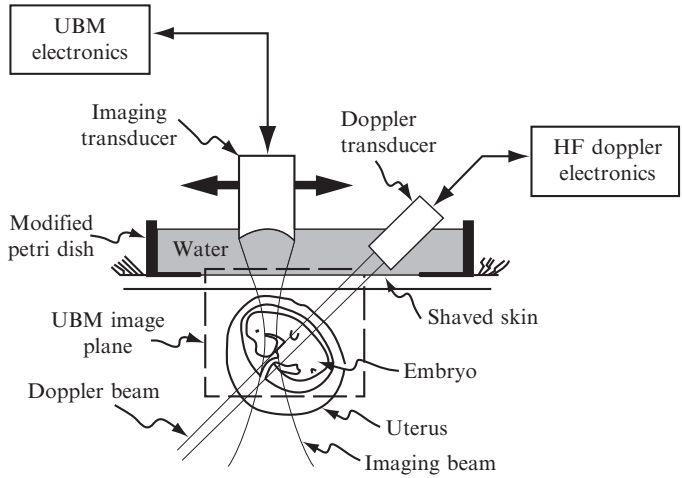

Figure 21.1 Schematic of setup for UBM analysis of mouse embryos. A pregnant mouse is anesthetized, the lower abdomen shaved, and the mouse is laid in the lower level of a two-level stage. A 100 mm plastic Petri dish with a 25 mm hole punched in the center is attached to the upper level and filled with water. The UBM and Doppler transducers are then scanned in the resulting water bath to acquire images and Doppler blood velocity waveforms. The temperature of the water and mouse are maintained at 37 °C with a feedback temperature controller for all physiological measurements. Reprinted with permission from Aristizabal *et al.* (1998).

pregnant mouse, remove the hair on the skin overlying the embryos, and couple the UBM transducer to the mouse using a commercially available ultrasound gel, or a holding system that incorporates a water bath between the transducer and the skin (Fig. 21.1). Two-dimensional (2D) UBM images are acquired in real time ($\geq$100 images/s with current technology), and 3D imaging can be accomplished by acquiring a stack of 2D UBM images (Aristizabal *et al.*, 2006). Recently, commercial UBM scanners have also included color flow imaging, in which Doppler signals are analyzed in real time to produce a color-coded map of blood velocities (Foster *et al.*, 2009).

To date, UBM has found greatest application in the mouse cardiovascular system, although similar techniques should provide data relevant to many organ systems. UBM and UBM–Doppler methods can be used over a very wide range of cardiovascular developmental stages (Fig. 21.2), from the onset of heart beat at E8.0 (Ji *et al.*, 2003), through the critical early stages of chamber formation between E10.5 and E14.5 (Phoon *et al.*, 2000, 2002; Srinivasan *et al.*, 1998; Zhou *et al.*, 2003), and into neonatal stages when cardiomyopathy and heart failure are first manifested in many mutants (Fatkin *et al.*, 1999). Interestingly, the first UBM studies for

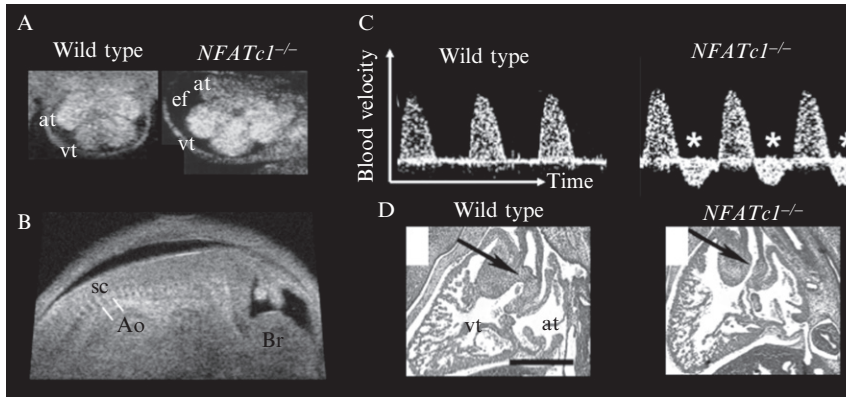

Figure 21.2 UBM analysis of cardiovascular defects in mouse embryos. (A) UBM provides *in utero* images of the E12.5 embryonic heart, enabling identification and dynamic analysis of the cardiac atria (at) and ventricles (vt), including detection of pericardial effusions in a subset of $NFATc1^{-/-}$ mutants. (B) UBM images were used to place the Doppler sample volume (hatch marks) over the aorta (Ao), to acquire blood velocity waveforms in E13.5 wild type and $NFATc1^{-/-}$ mutants (C). Doppler analysis showed clear evidence of regurgitant flow patterns (*) in the mutants resulting from defects in aortic valve formation (arrows; D). Other labels: Br, brain; sc; spinal cord. Panels (A), (C), and (D) reprinted with permission from Phoon *et al.* (2004).

phenotyping $NFATc1^{-/-}$ mutants, which lack aortic and pulmonary cardiac valves and die *in utero*, revealed unusual mechanisms of embryonic heart failure (Phoon *et al.*, 2004). Longitudinal studies of each embryo in a pregnant mouse, required for effective *in utero* phenotype analysis with UBM, is challenging but can be achieved through careful mapping of extra- and intraembryonic anatomical landmarks to enable accurate identification of individual embryos over a period of several days (Ji and Phoon, 2005).

2.2. *In utero* UBM-guided injections

For over a decade, UBM has provided a unique and powerful approach for direct *in utero* image-guided manipulation of mouse embryos (Liu *et al.*, 1998; Olsson *et al.*, 1997). This has been most utilized in the developing embryonic brain, where UBM-guided injections have enabled *in utero* neural cell transplantation (Butt *et al.*, 2005; Olsson *et al.*, 1997; Wichterle *et al.*, 2001), cell lineage tracing (Kimmel *et al.*, 2000), and gain-of-function studies with retroviruses or electroporation (Gaiano *et al.*, 1999; Punzo and Cepko, 2008; Weiner *et al.*, 2002). For UBM-guided injections, timed pregnant mice are anesthetized with nembutol or isoflurane, and the uterus exposed after laparotomy (Fig. 21.3). Hair is

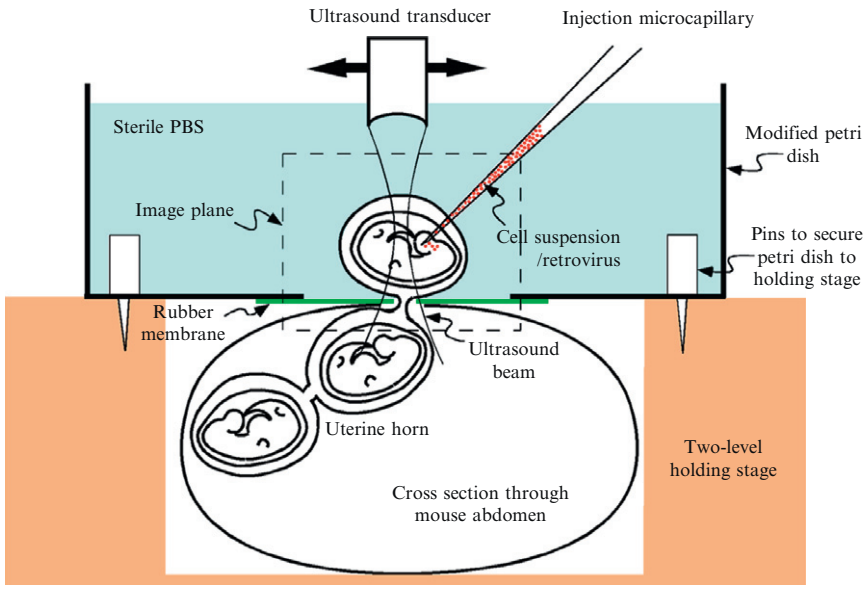

Figure 21.3 Schematic of setup for UBM-guided injections. A pregnant mouse is anesthetized, the abdomen shaved, and a midline incision made through the skin and muscle to gain access to the uterine horn. The mouse is laid in the lower level of a two-level stage, with a modified Petri dish attached to the upper level. Part of the uterus containing a single embryo is gently pulled through a slot in a thin rubber membrane, into a bath of sterile PBS for injection under real-time UBM image guidance. Reprinted with permission from Liu *et al*. (1998).

removed from the lower abdominal skin, and a midline incision made through the skin and peritoneum. The pregnant mouse is laid supine in the lower section of a two-level stage, and a plastic Petri dish, modified by punching a ~25 mm diameter central hole, is secured over her abdomen. Part of the uterus containing one to two embryos (depending on embryonic stage) is gently pulled through a slot, cut into a thin rubber membrane stretched across the hole in the Petri dish, into sterile PBS. The UBM transducer is then lowered into the PBS bath, providing real-time imaging of the mouse brain and image-guidance of a pulled and sharpened 50-μm diameter glass microcapillary injection needle, mounted on a 3D micromanipulator and inserted through the uterine wall and into the embryonic target region (Fig. 21.4). After injection, one to two new embryos are gently pulled into the PBS, and the injected embryos gently placed back through the slot into the abdominal cavity. In this way, an entire litter (8–10 embryos) can be injected in ~1 h, after which the muscle and skin are sutured or clipped and the pregnant mouse recovers in a warming chamber until regaining consciousness. Like most surgical

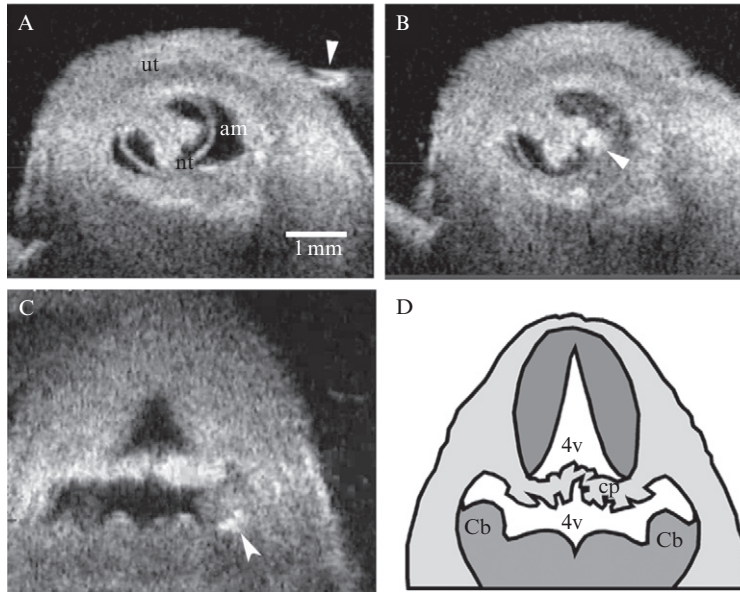

Figure 21.4 UBM-guided injections of the embryonic mouse nervous system. (A, B) At E8.5 the needle tip (arrows) is shown before (A) and after (B) insertion through the uterus (ut) and amniotic membrane (am) to inject a retrovirus adjacent to the (open) neural tube (nt). (C, D) At E13.5 a similar approach is used to inject a *Shh*-expressing retrovirus into the cerebellar anlage (Cb), which is easily identified from its lateral position in the mid-hindbrain, near the fourth ventricle (4v) and choroid plexus (cp). Panels (A) and (B) reprinted with permission from Gaiano *et al*. (1999); panels (C) and (D) reprinted with permission from Weiner *et al*. (2002).

procedures, survival of embryos is operator-dependent, but most people can achieve at least 50–60% embryonic survival after practice, and many can reach 80% survival or better for *in utero* brain injections. In addition to the applications described above, UBM-guided injection can also provide a unique method for precise targeting of cell-labeling agents in mouse embryos, for example, with MRI contrast agents that label cells that can then be followed with longitudinal MRI imaging.

3. Magnetic Resonance Microimaging

MRI is well-established in clinical radiology as an imaging tool that provides excellent soft tissue contrast for isolating pathologies or characterizing anatomy. Increasingly, MRI is also used for assessment of functional parameters, such as blood perfusion, oxygenation status, or cardiac

dynamics, and in larger population studies to identify regions altered by disease or development (Aljabar *et al.*, 2008; Davatzikos *et al.*, 2005; Janke *et al.*, 2001). MRI, like ultrasound, can be scaled down for magnetic resonance microimaging (micro-MRI), providing a powerful quantitative approach for assessing changes in 3D anatomy and physiology during development, including isolating phenotypes in genetically modified mice.

Compared to UBM, micro-MRI image contrast is remarkably flexible, allowing optimization of image acquisition to highlight anatomy or pathology of interest. The MRI signal is ultimately derived from the perturbed magnetic state of water protons within the tissue; however, variations in the acquisition can emphasize image contrast from different physical processes affecting the proton signal. Traditional images are referred to as proton-density-, T_1-, or T_2-weighted images, according to the mechanism most reflected in the image contrast. However, diffusion, perfusion, blood flow or macromolecular content can also provide a basis for image contrast, and may be preferred in many applications in developmental biology studies. Administration of contrast agents that produce hyper- or hypointensity in an image is also prevalent, and particularly common in mouse imaging, both for *in vivo* and *ex vivo* imaging studies. This contrast flexibility provides opportunities in research to highlight physiology, anatomy, and even molecular/cellular regions of interest.

Typical resolutions achieved with *in vivo* micro-MRI are on the order of 100 μm in adult mice. The reduced size of the embryo, particularly during early developmental stages, requires higher resolution for visualization of anatomical features. This limitation has meant that MRI imaging has been most feasible in mid- to late-embryonic stages, starting around E12. Likewise, there has been a preference for studying embryos with *ex vivo* micro-MRI, where specimen imaging hardware and longer acquisition times can be tailored to achieve the necessary resolution increase without the concerns for anesthesia and animal maintenance necessary *in vivo*. Nevertheless, *in vivo* micro-MRI methods are particularly beneficial for examining early-postnatal mice, when the phenotype permits, and continued development of *in utero* imaging methods shows potential for more widespread *in utero* studies in the future.

Below we describe methods for both *ex vivo* and *in vivo* micro-MRI of mouse development (Turnbull and Mori, 2007). Developmental MRI studies to date have focused primarily on the heart, brain, or vascular systems and so these areas are highlighted in this chapter. This is, however, in part a reflection of the developmental biology community at large and should not be considered an inherent limitation of the technology. Indeed, with a high demand for phenotyping mice, and a large number of embryonic lethal phenotypes, continued development of embryo phenotyping tools will remain a priority.

3.1. *Ex vivo* anatomical micro-MRI

Although one of the frequently cited benefits of MRI is its *in vivo* potential, *ex vivo* images provide exquisite spatial resolution for detection of phenotypes at defined time points. This permits a more detailed anatomical comparison between mutant and wild-type groups for detection of subtle phenotypes. *Ex vivo* images generally run for many hours in an ''overnight'' scan session, achieving spatial resolutions between 20 and 50 μm. These images can be acquired on a routine basis, and are highly appropriate for screening new mutants and performing volumetric structural analyses of phenotypes (Fig. 21.5; Petiet *et al.*, 2008).

Ex vivo imaging requires fixation and mounting of embryonic specimens for micro-MRI. Mouse embryos are harvested at a defined stage, where by convention noon of the day after mating is defined as embryonic day 0.5 (E0.5). After extraction from the uterus, embryos are immersed overnight or longer in 4% paraformaldehyde (PFA) or equivalent for fixation at 4 °C. For mid- to late-stage embryos, embryos can also be perfusion-fixed for improved fixation, and for vascular imaging, as described below. Prior to imaging, specimens are embedded in 1–3% agar or immersed in a proton-free fluid, such as Fomblin (Ausimount) or Fluorinert (3 *M*). Some investigators also report ''doping'' the agar either proton-free fluid or an iron-oxide contrast agent in order to reduce the background agar signal in the image (Dhenain *et al.*, 2001).

For imaging, prepared sample tubes are placed within radiofrequency coils that collect the proton signal used to reconstruct images. Small solenoid coils ($\sim$10 mm diameter, $\sim$15 mm length) that fit closely around individual sample tubes provide optimal detection of the water proton signal and signal-to-noise ratio, a common metric of image quality. However, high-resolution *ex vivo* scans commonly require many hours and are run in ''overnight'' scan sessions, so imaging one embryo per evening can be prohibitively slow. In the aim of increasing throughput, multiple samples can be embedded in larger tubes and placed in a single larger coil, and then imaged collectively (Schneider *et al.*, 2004). This results in one large image, from which individual, 3D images containing single specimens can be extracted. An alternative method for increasing throughput is offered in specialized MRI systems equipped for multiple-mouse MRI (Bock *et al.*, 2003). This technology enables many imaging experiments to be run in parallel, utilizing several single-specimen solenoid coils with one specimen each and avoiding any compromise in image quality—an unavoidable consequence of using a single larger coil.

With either hardware configuration, image acquisition must be prescribed to achieve the desired contrast. It is common to perform a refinement of imaging parameters to achieve the contrast optimal for a particular application. For general anatomical discrimination at high-field ($\geq$7 T),

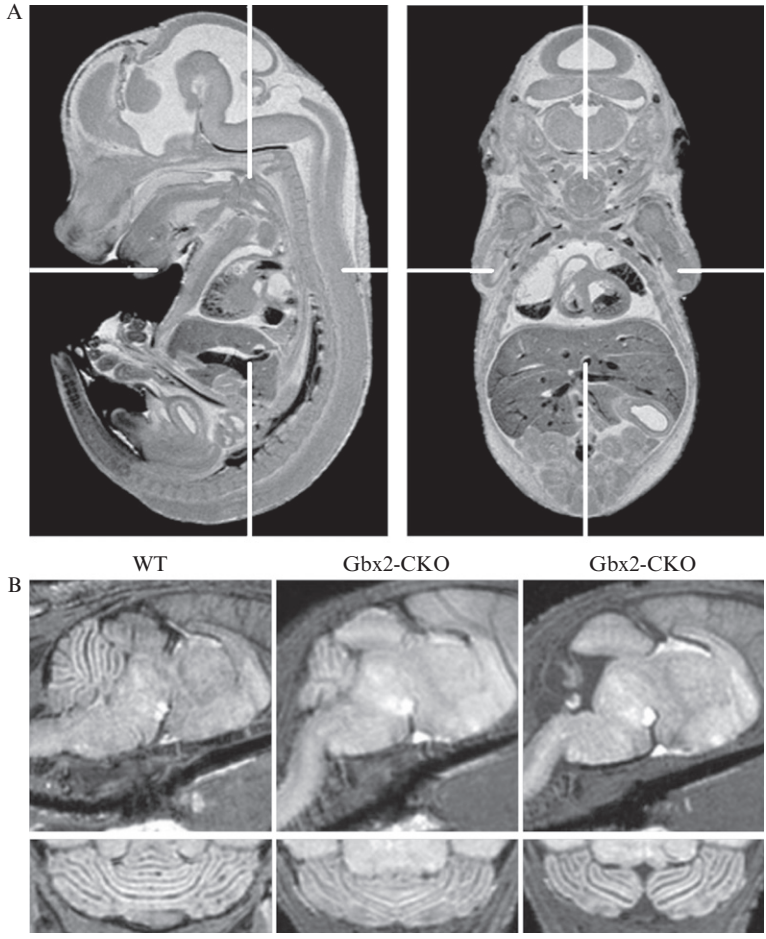

Figure 21.5 Anatomical micro-MRI in the mouse embryo and neonate. High-resolution, 3D images, such as the example in (A) in an E15.5 fixed mouse embryo, provide excellent anatomical detail for phenotyping. *In vivo* anatomical phenotyping is also possible, especially during early-postnatal development. One example is provided in (B), showing variable cerebellar defects in *Gbx2* conditional knockout mice on postnatal day P11. At left, is shown a wild-type mouse in sagittal (top) and horizontal (bottom) views. The second and third columns show a mild and severe example of the cerebellar defect. Panels (A) and (B) reprinted from Petiet *et al*. (2008) and Wadghiri *et al*. (2004), respectively with permission.

T_2-weighted imaging is generally preferred (Dhenain *et al*., 2001), and can be achieved in fixed samples using repetition time (TR) $\geq$2000 ms and echo time (TE) $\sim$35 ms. Improved acquisition efficiency can be achieved by adding modest concentrations of MRI contrast agent—most commonly

gadolinium compounds such as DTPA-Gd or DOTA-Gd—to the fixative and storage solutions. This serves to increase the rate of water proton signal dynamics, thereby allowing for either shorter imaging sessions or higher resolution images. A concentration of 2 m*M* Gd-chelate in the fixative, for instance, in combination with TR $\sim$ 300 ms and TE $\sim$ 35 ms retains excellent T_2-weighted contrast in a fraction of the acquisition time. Alternatively, more highly doped samples (with $\geq$30 m*M* Gd-chelate, for instance) may allow more rapid imaging (Johnson *et al.*, 2007), with TR and TE reduced to $\sim$50 and $\sim$5 ms. In the latter case, contrast is heavily dependent on contrast agent distribution and diligence ensuring consistent specimen preparation is paramount. Modest concentrations of contrast agent ($\leq$3 m*M* Gd-chelate) are also beneficial for diffusion tensor imaging (described below), but higher concentrations confound measurements of the diffusion related signal effects.

Methods for evaluating mouse embryo development with *ex vivo* micro-MRI have been available for over a decade (Smith *et al.*, 1996), with continued improvements resulting in atlases of mouse development from as early as E6.5, and with resolutions $\sim$20 μm (Dhenain *et al.*, 2001; Petiet *et al.*, 2008). Micro-MRI shows potential for phenotyping of embryos in developmental studies (Schneider *et al.*, 2003b), and has been particularly successful in studying cardiac morphology and structure (Smith, 2001). The heart, with its several chambers and intertwining inflow and outflow tracts, is a structure that can be very difficult to appreciate using traditional histological sections and is best-visualized with 3D imaging methods. These features have been helpful in phenotyping of the *Cited2* and *Cx43* mutants, identifying atrial and ventricular septal defects, inflow and outflow tract abnormalities, and aortic arch malformations (Schneider *et al.*, 2003a; Wadghiri *et al.*, 2007). Phenotyping has also been performed in the brain, revealing changes associated with ethanol or retinoic acid administration during pregnancy (Parnell *et al.*, 2009), and a preliminary study investigating study of bone development has also been reported (Ichikawa *et al.*, 2004).

Despite these successes, micro-MRI for study in development has not been used as widely as might be expected. MR scanner availability and challenges associated with analyzing large 3D image data sets in a systematic and efficient way have likely been among the historical barriers. In this regard, analysis of the resulting images for possible phenotypes is a crucial step, one that cannot be treated fully here. The processing steps depend largely on the phenotypes in question. Anatomical phenotypes remain the most commonly investigated by micro-MRI and are appropriate for initial investigations and general characterizations of new mutants. Gross phenotypes can be detected by simple inspection of images, and are of sufficient severity that further analysis provides little additional insight. In many instances, more subtle anatomical differences are present. In these cases, segmentation of structural volumes or computational analysis of local

volume/shape changes is necessary to describe the anatomical phenotype. These analysis methods, while employed extensively in adult mouse brain, have had more limited application in developmental studies. However, the tools are not inherently limited to adults, and are beginning to be applied more widely in the embryo and neonate as imaging methods are refined. In general, anatomical phenotypes are very common in genetic mutants (Nieman *et al.*, 2007), so results are likely to be plentiful and micro-MRI provides an important starting point for further investigation.

3.2. *Ex vivo* diffusion tensor imaging

Some anatomical features in embryos, particularly in the central nervous system, are difficult to visualize with traditional MRI contrast weighting. White matter, for instance, which exhibits prominent contrast in later stages, is still under development in embryonic stages so that brain structures myelinated in the adult can be difficult to visualize in the embryonic brain. Novel contrast mechanisms based on water diffusion properties enable enhanced contrast of these structures, and further—through a method called diffusion tensor imaging (DTI)—provide data for computation of the preferential diffusion directions associated with the presence of axons or other anisotropic structures. DTI methods can be used in the postnatal human brain, and show great potential for MR-based phenotyping in the embryonic mouse brain.

DTI data is generally computed based on a set of six or more diffusion-weighted images in addition to a reference, minimally diffusion-weighted (e.g., T_2-weighted) image. The degree of diffusion weighting is controlled in the scan by adjusting a parameter called the *b*-value. Diffusion-weighted images are typically acquired with $b = 1000$–1500 s/mm^2. The low diffusion reference image is generally acquired with a nominal value of $b = 0$ s/mm^2, although higher values ($b \sim 200$ s/mm^2) have been used in fixed samples where some suppression of background signal from the embedding medium is desirable (Mori *et al.*, 2001). As each separate diffusion-weighted image requires as long or longer than an individual anatomical image (such as a T_2-weighted image), acquisition time in DTI studies is often a limiting factor.

The fixation of embryos for DTI–MRI may be performed as described above for standard *ex vivo* imaging. The use of contrast agents during fixation can also be beneficial for speeding image acquisition, but only modest concentrations (≤ 3 m*M* Gd-chelate) are appropriate as high concentrations of contrast agents may confound measurements of the diffusion related signal effects. While absolute measures of diffusion measured in fixed specimens differ from measurements in the *in vivo* case (Shepherd *et al.*, 2009; Sun *et al.*, 2009), relative measures including the principal diffusion directions are not altered (Kim *et al.*, 2009; Sun *et al.*, 2003).

After collection of the necessary images, it is common to process the images to produce a map representing diffusion properties in the brain. In the simplest case, a map showing the degree of anisotropy—the extent to which there is a preferred diffusion direction—can be produced and shown in a simple gray scale image, providing a novel anatomical map emphasizing structures altering water diffusion. To show the principle diffusion direction on DTI images, a color map convention for visualization of DTI data sets has emerged in which the medial–lateral, dorsal–ventral, and rostral–caudal directions are each represented as one of the red, green, or blue channels in an RGB color space. The intensity of the colors can then be modulated by the degree of anisotropy, fading to black for isotropic diffusion and appearing at full intensity for directional diffusion. Both MRI system manufacturer and independent software is available for the computation of the DTI maps from the raw diffusion-weighted imaging data.

DTI maps are particularly powerful for micro-MRI of mouse brain development (Fig. 21.6). Defects in the formation of key white matter structures including the corpus callosum and the hippocampal commissure, as in *Robo1* and *Netrin1* mutants, can be analyzed (Andrews *et al.*, 2006; Zhang *et al.*, 2003). Similarly, apparent degeneration of white matter structures—the fimbria and commissures—has been reported during postnatal development (Zhang *et al.*, 2005a). In addition to enhancing white matter conspicuity, DTI maps also provide surprising contrast in the neocortex of developing embryos (Mori *et al.*, 2001). Methods for automated analysis based on diffeomorphic mapping in DTI-derived maps have also been reported (Zhang *et al.*, 2005b), suggesting routine automated screening and analysis could be developed.

3.3. *Ex vivo* vascular imaging

A sensitive method for vascular imaging in *ex vivo* embryo specimens requires perfusion with an intravascular contrast agent, such as DTPA-Gd conjugated to albumen. For this, the umbilical vessels are isolated for cannulation and perfusion–fixation after exteriorizing the embryo from the uterus and yolk sac (Smith *et al.*, 1994, 1996). The intravascular contrast agent is mixed in gelatin solution and perfused into the embryo after flushing the blood and fixative solutions, after which the umbilical vessels are tied off and the embryo is further immersion fixed as described above (without contrast agent). Imaging then proceeds with a T_1-weighted imaging sequence (TR $\leq$ 50 ms; TE $\leq$ 5 ms), producing bright blood vessels in the presence of the intravascular contrast agent (Fig. 21.7).

The benefit of 3D imaging is particularly important for analysis of the vascular system. The branching, tree-like structure of the vasculature cannot be captured in 2D histological sections, making 3D methods a necessity. In some cases, important findings can be overlooked in traditional histology

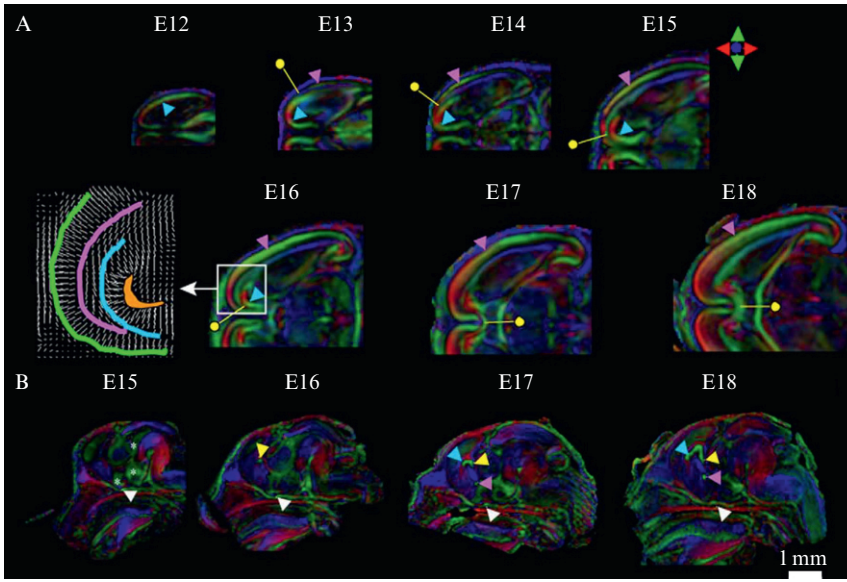

Figure 21.6 Diffusion tensor imaging in the developing mouse brain. Diffusion tensor data is shown with a color map, where red, green, and blue each represent diffusion in an orthogonal direction as indicated by the arrows. In panel (A), horizontal images from E12 to E18 are provided. Pink and blue arrowheads represent the cortical plate and neuroepithelium, respectively. Yellow pins indicate the leading edge of the growing intermediate zone. A white box is expanded at E16 to show the fiber orientation in a vector picture. In panel (B), the equivalent sagittal images are provided for E15–E18. In this case, white, yellow, pink, and blue arrowheads indicate the optic chiasm, hippocampal commissure, anterior commissure, and corpus callosum, respectively. Asterisks (*) mark the neuroepithelium around the third ventricle. All data are from full three-dimensional data sets. Reprinted from Zhang *et al.* (2003) with permission.

or pathology due to the difficulty in assessing the entire vascular tree. For example, the deletion of basilar artery in *Gli2*$^{-/-}$ mutants was only noticed during micro-MRI analysis (Fig. 21.7; Berrios-Otero *et al.*, 2009). Similarly, micro-MRI of *Connexin43* mutant mice revealed abnormal development of both the right ventricle and major outflow tracts, difficult to appreciate from histological analysis (Huang *et al.*, 1998; Wadghiri *et al.*, 2007).

3.4. *In vivo* micro-MRI of mouse embryos and neonates

In vivo micro-MRI offers unique opportunities to assess longitudinal development and functional parameters such as blood perfusion, heart motion, or other physiological measures. *In vivo* studies can also be convenient in the context of comprehensive phenotyping studies, in which several additional

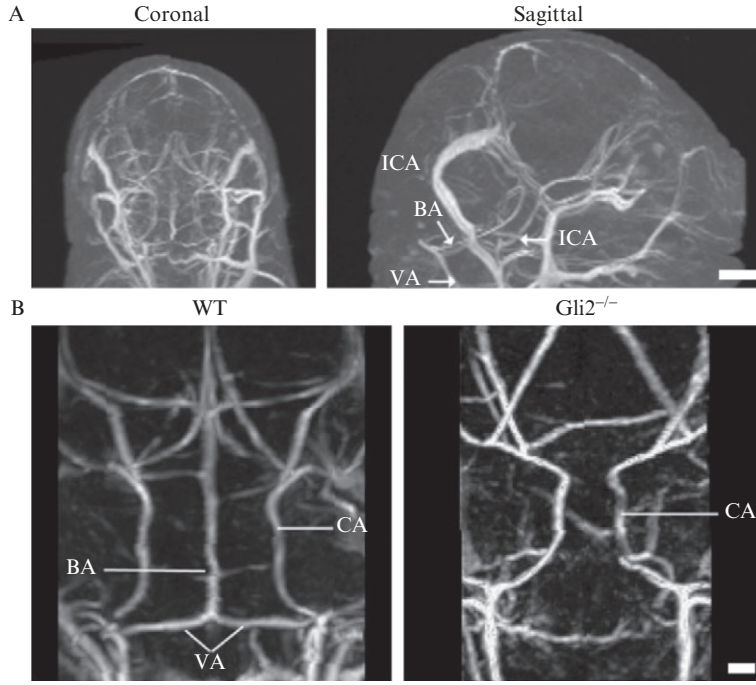

Figure 21.7 *Ex vivo* imaging of embryo vasculature. In panel (A), maximum intensity projections through an E15.5 embryo data set are shown in two orthogonal planes. The internal carotid arteries (ICA), vertebral arteries (VA), and basilar artery (BA) are labeled. In panel (B), comparison of wild type and Gli2$^{-/-}$ embryos at E17.5 reveals a missing basilar artery in the mutant. Reprinted from Berrios-Otero *et al.* (2009) with permission.

assays are required following initial imaging assessment, or in the case of conditional mutants, where variably penetrant phenotypes motivate detailed, time course imaging of individual animals. However, *in vivo* micro-MRI during development has been historically challenging. The small size of embryonic and neonatal mice requires high-resolution images, and consequently long scan times. The mice must be anesthetized throughout this period, and physiological monitoring and peripheral heating must be employed to ensure proper maintenance of their health. Physiological and other motion during the scans—detrimental to image quality—must be eliminated or compensated.

In vivo micro-MRI has been applied successfully in neonatal mice. Although the small size of neonates makes positioning and restraint challenging, good results can be achieved provided dedicated neonate cradles and setups similar to those used for adult mouse imaging. Isoflurane gas is the preferred method of anesthesia. After induction at 4–5%, animals can be

maintained at ~1% isoflurane concentration for extended time periods (up to ~3 h). During this time, body temperature should be maintained with external heat sources and physiological signs must be monitored. Small ECG electrodes have been employed in mice as early as 3 days after birth, timing the acquisition of MRI data to the phase of the heart cycle to allow excellent visualization of the heart via prospectively gated cine-MRI methods (Wiesmann *et al.*, 2000). Despite these successes, physiological monitoring can be a challenging aspect of working with neonates. Detection of respiratory or cardiac events using additional data acquired from the MRI scanner itself has been shown as an alternate method for detection of physiological events, and in our experience can greatly improve the efficiency of setup for neonate imaging, without compromising monitoring capability during the 3D imaging session (Nieman *et al.*, 2009). Repeated *in vivo* imaging of individual mice postnatally provides a measure of brain development, mapping regions of the most rapid growth quantitatively (Fig. 21.8). Longitudinal growth maps through several time points can provide a quantitative picture of the growth process from birth through adulthood. Comparisons of *in vivo* images of neonatal mice with different genotypes have also demonstrated potential for phenotyping, visualizing, for instance, abnormalities in the *Gbx2* mutant cerebellum (Fig. 21.5; Wadghiri *et al.*, 2004).

Imaging the embryo *in utero* has been more limited, largely because it is not possible to reliably keep the embryo from moving inside the maternal abdomen. While neonates—with extra care and dedicated hardware—can be handled with similar procedures as adult animals, embryos *in utero* cannot be

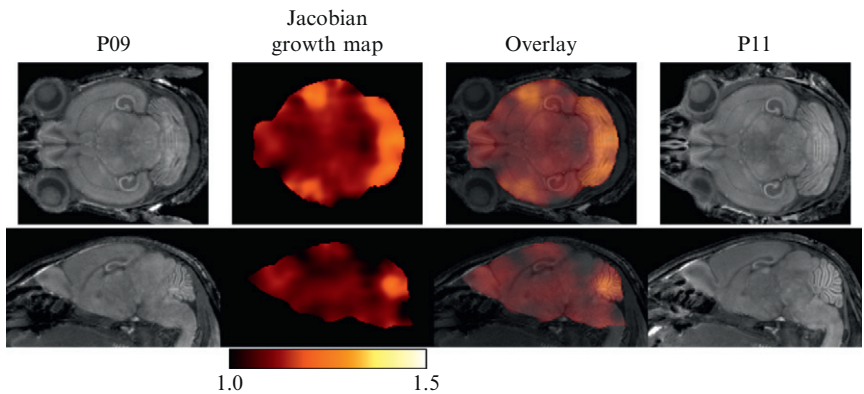

Figure 21.8 Computational mapping of growth in the developing mouse brain. *In vivo* Mn-enhanced MRI images at days 9 and 11 after birth (left and rightmost columns, respectively) provide a visual representation of growth-related changes. Computational image processing can provide a quantitative growth map (second column). An overlay of the growth map on the outline of the P09 mouse shows that the most significant growth is occurring in the cerebellum and regions of the cortex.

restrained or monitored in the same fashion. One solution to this challenge is to image more quickly, using rapid acquisition of 2D slices rather than acquisition of high-resolution 3D volumes. This method has been applied successfully by several groups (Chapon *et al.*, 2002; Hogers *et al.*, 2000) using a T_2-weighted spin-echo imaging sequence, including one example in which *in utero* imaging could distinguish between genotypes in embryos transgenically expressing human ferritin (Cohen *et al.*, 2007). However, the 2D rapid MR images provide very limited image detail and lack sufficient anatomical data to investigate any but the most obvious phenotypes.

Imaging methods that permit acquisition of high-resolution 3D volumes in the presence of motion should permit much improved study of the live embryo *in utero*. In late-embryonic stages, where the resolution capabilities of MRI may be satisfactory, movement is somewhat restricted relative to earlier stages, so only a small amount of motion need be accounted for. We have found that gating on maternal respiratory motion, in combination with manganese (Mn) enhancement via maternal i.p. injection of $MnCl_2$, can provide high-quality *in utero* T_1-weighted images, enabling volumetric analysis of ventral forebrain defects in *Nkx2.1*$^{-/-}$ mutant embryos (Deans *et al.*, 2008). For additional motion compensation, prescription of a series of rapid 3D volume acquisitions (with 3–5 min acquisition time per image) provides images with sufficient quality to detect image motion between serially acquired images. In postprocessing, therefore, a set of serial images can be corrected for motion and then combined to produce high-quality image reconstructions. In combination with detection of cardiac motion, we have shown that this method can even be used to produce images of the beating embryonic heart (Fig. 21.9; Nieman *et al.*, 2009).

Further improvements for *in utero* imaging will broaden the potential application of these emerging methods. Most notably, dedicated hardware configurations for *in utero* imaging will be necessary to enhance imaging results sufficiently for routine application. Dedicated coil arrays, for instance, may improve the imaging outcome, allowing large field-of-view pilots to isolate individual embryos and yet still offer the sensitivity of a small surface coil for small field-of-view embryo imaging. Isotropic resolution close to 70 μm would likely be sufficient for many developmental studies, commencing in mid- to late-embryonic stages. Nonetheless, the complications associated with *in utero* imaging will mean it is not likely to serve the same screening role as *ex vivo* imaging, but will rather be used for assessing particular phenotypes requiring longitudinal examination. Important applications for *in utero* imaging include the evaluation of developmental changes that occur between late-embryonic and early-postnatal stages, functional measurements (such as cardiac performance or blood perfusion) in embryos with mutations lethal in late-embryonic stages, and time course studies of developmental abnormalities during maternal exposure to toxins.

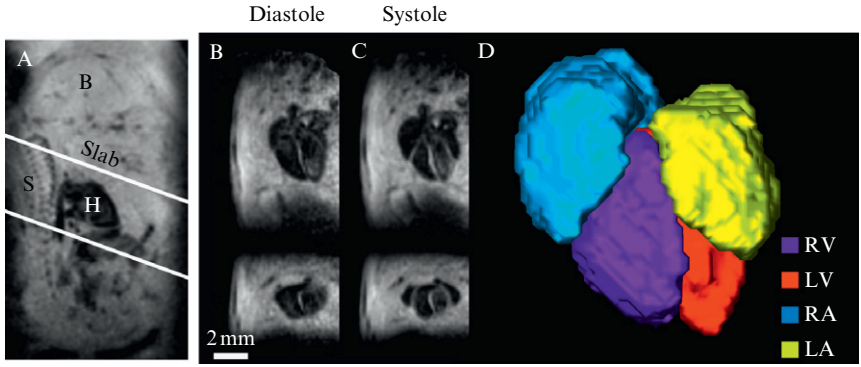

Figure 21.9 *In utero* MRI of the beating embryonic heart. With appropriate motion-correction, it is possible to image a volume (depicted in as an imaging slab in (A)) including the embryonic heart (day E17). Orthogonal long- and short-axis views are shown at diastole in (B) and (C). A volumetric rendering of the four heart chambers in (D) emphasizes the three-dimensional character of the data and shows the similarity in the four chamber volumes. Reprinted from Nieman *et al.* (2009) with permission.

4. Summary

UBM and micro-MRI are microimaging techniques based on ultrasound and magnetic resonance, respectively, that provide powerful new approaches for anatomical and functional phenotype analysis in developing mouse embryos and neonates. UBM provides real-time image acquisition and Doppler blood velocity measurements, which has been widely used for studies of brain and cardiovascular development, and as a method for *in utero* image-guided injections. Micro-MRI has more flexibility for image contrast compared to UBM, but requires longer acquisition times. Micro-MRI of multiple fixed mouse embryos can be applied in a relatively high-throughput manner, with and without contrast agents, to analyze a wide range of phenotypes. In addition to these more conventional MRI methods, diffusion-weighted MRI and DTI have been demonstrated for 3D analysis of tissue microstructure and connectivity that is difficult to appreciate with standard histological analysis. Finally, recent advances have shown the feasibility of using micro-MRI for *in utero* imaging in live mouse embryos, providing the potential for future longitudinal studies of individual mice from embryonic to adult stages.

ACKNOWLEDGMENTS

We thank Drs. Allan Johnson (Duke University), Susumu Mori (Johns Hopkins University), and Collin Phoon (New York University School of Medicine) for permission to reprint

figures from their published work. We are grateful to all our current and past students, postdocs, and colleagues at the Mouse Imaging Centre and the Skirball Institute of Biomolecular Medicine who contributed to the work described in this chapter. We especially thank Kamila Szulc who provided the micro-MRI data used to compute the developmental growth map shown in Fig. 21.8. Some of the research described in this chapter was supported by grants from the National Institutes of Health (R01 NS038461, R01 HL078665) and contracts from the New York State Department of Health (C022053, C020926).

REFERENCES

Aljabar, P., Bhatia, K. K., Murgasova, M., Hajnal, J. V., Boardman, J. P., Srinivasan, L., Rutherford, M. A., Dyet, L. E., Edwards, A. D., and Rueckert, D. (2008). Assessment of brain growth in early childhood using deformation-based morphometry. *Neuroimage* **39,** 348–358.

Andrews, W., Liapi, A., Plachez, C., Camurri, L., Zhang, J., Mori, S., Murakami, F., Parnavelas, J. G., Sundaresan, V., and Richards, L. J. (2006). Robo1 regulates the development of major axon tracts and interneuron migration in the forebrain. *Development* **133,** 2243–2252.

Aristizabal, O., Christopher, D. A., Foster, F. S., and Turnbull, D. H. (1998). 40-MHz echocardiography scanner for cardiovascular assessment of mouse embryos. *Ultrasound Med. Biol.* **24,** 1407–1417.

Aristizabal, O., Ketterling, J. A., and Turnbull, D. H. (2006). 40-MHz annular array imaging of mouse embryos. *Ultrasound Med. Biol.* **32,** 1631–1637.

Berrios-Otero, C. A., Wadghiri, Y. Z., Nieman, B. J., Joyner, A. L., and Turnbull, D. H. (2009). Three-dimensional micro-MRI analysis of cerebral artery development in mouse embryos. *Magn. Reson. Med.* **62,** 1431–1439.

Bock, N. A., Konyer, N. B., and Henkelman, R. M. (2003). Multiple-mouse MRI. *Magn. Reson. Med.* **49,** 158–167.

Butt, S. J., Fuccillo, M., Nery, S., Noctor, S., Kriegstein, A., Corbin, J. G., and Fishell, G. (2005). The temporal and spatial origins of cortical interneurons predict their physiological subtype. *Neuron* **48,** 591–604.

Chapon, C., Franconi, F., Roux, J., Marescaux, L., Le Jeune, J. J., and Lemaire, L. (2002). In utero time-course assessment of mouse embryo development using high resolution magnetic resonance imaging. *Anat. Embryol. (Berl.)* **206,** 131–137.

Cohen, B., Ziv, K., Plaks, V., Israely, T., Kalchenko, V., Harmelin, A., Benjamin, L. E., and Neeman, M. (2007). MRI detection of transcriptional regulation of gene expression in transgenic mice. *Nat. Med.* **13,** 498–503.

Davatzikos, C., Shen, D., Gur, R. C., Wu, X., Liu, D., Fan, Y., Hughett, P., Turetsky, B. I., and Gur, R. E. (2005). Whole-brain morphometric study of schizophrenia revealing a spatially complex set of focal abnormalities. *Arch. Gen. Psychiatry* **62,** 1218–1227.

Deans, A. E., Wadghiri, Y. Z., Berrios-Otero, C. A., and Turnbull, D. H. (2008). Mn enhancement and respiratory gating for in utero MRI of the embryonic mouse central nervous system. *Magn. Reson. Med.* **59,** 1320–1328.

Dhenain, M., Ruffins, S. W., and Jacobs, R. E. (2001). Three-dimensional digital mouse atlas using high-resolution MRI. *Dev. Biol.* **232,** 458–470.

Fatkin, D., Christe, M. E., Aristizabal, O., McConnell, B. K., Srinivasan, S., Schoen, F. J., Seidman, C. E., Turnbull, D. H., and Seidman, J. G. (1999). Neonatal cardiomyopathy in mice homozygous for the Arg403Gln mutation in the alpha cardiac myosin heavy chain gene. *J. Clin. Invest.* **103,** 147–153.

Foster, F. S., Mehi, J., Lukacs, M., Hirson, D., White, C., Chaggares, C., and Needles, A. (2009). A new 15–50 MHz array-based micro-ultrasound scanner for preclinical imaging. *Ultrasound Med. Biol.* **35,** 1700–1708.

Gaiano, N., Kohtz, J. D., Turnbull, D. H., and Fishell, G. (1999). A method for rapid gain-of-function studies in the mouse embryonic nervous system. *Nat. Neurosci.* **2,** 812–819.

Hogers, B., Gross, D., Lehmann, V., Zick, K., De Groot, H. J., Gittenberger-De Groot, A. C., and Poelmann, R. E. (2000). Magnetic resonance microscopy of mouse embryos in utero. *Anat. Rec.* **260,** 373–377.

Huang, G. Y., Wessels, A., Smith, B. R., Linask, K. K., Ewart, J. L., and Lo, C. W. (1998). Alteration in connexin 43 gap junction gene dosage impairs conotruncal heart development. *Dev. Biol.* **198,** 32–44.

Ichikawa, Y., Sumi, M., Ohwatari, N., Komori, T., Sumi, T., Shibata, H., Furuichi, T., Yamaguchi, A., and Nakamura, T. (2004). Evaluation of 9.4-T MR microimaging in assessing normal and defective fetal bone development: Comparison of MR imaging and histological findings. *Bone* **34,** 619–628.

Janke, A. L., de Zubicaray, G., Rose, S. E., Griffin, M., Chalk, J. B., and Galloway, G. J. (2001). 4D deformation modeling of cortical disease progression in Alzheimer's dementia. *Magn. Reson. Med.* **46,** 661–666.

Ji, R. P., and Phoon, C. K. (2005). Noninvasive localization of nuclear factor of activated T cells c1−/− mouse embryos by ultrasound biomicroscopy-Doppler allows genotype-phenotype correlation. *J. Am. Soc. Echocardiogr.* **18,** 1415–1421.

Ji, R. P., Phoon, C. K., Aristizabal, O., McGrath, K. E., Palis, J., and Turnbull, D. H. (2003). Onset of cardiac function during early mouse embryogenesis coincides with entry of primitive erythroblasts into the embryo proper. *Circ. Res.* **92,** 133–135.

Johnson, G. A., Ali-Sharief, A., Badea, A., Brandenburg, J., Cofer, G., Fubara, B., Gewalt, S., Hedlund, L. W., and Upchurch, L. (2007). High-throughput morphologic phenotyping of the mouse brain with magnetic resonance histology. *Neuroimage* **37,** 82–89.

Kim, T. H., Zollinger, L., Shi, X. F., Rose, J., and Jeong, E. K. (2009). Diffusion tensor imaging of ex vivo cervical spinal cord specimens: The immediate and long-term effects of fixation on diffusivity. *Anat. Rec. (Hoboken)* **292,** 234–241.

Kimmel, R. A., Turnbull, D. H., Blanquet, V., Wurst, W., Loomis, C. A., and Joyner, A. L. (2000). Two lineage boundaries coordinate vertebrate apical ectodermal ridge formation. *Genes Dev.* **14,** 1377–1389.

Lerch, J. P., Carroll, J. B., Spring, S., Bertram, L. N., Schwab, C., Hayden, M. R., and Henkelman, R. M. (2008). Automated deformation analysis in the YAC128 Huntington disease mouse model. *Neuroimage* **39,** 32–39.

Liu, A., Joyner, A. L., and Turnbull, D. H. (1998). Alteration of limb and brain patterning in early mouse embryos by ultrasound-guided injection of Shh-expressing cells. *Mech. Dev.* **75,** 107–115.

Marxen, M., Thornton, M. M., Chiarot, C. B., Klement, G., Koprivnikar, J., Sled, J. G., and Henkelman, R. M. (2004). MicroCT scanner performance and considerations for vascular specimen imaging. *Med. Phys.* **31,** 305–313.

Metscher, B. D. (2009). MicroCT for developmental biology: A versatile tool for high-contrast 3D imaging at histological resolutions. *Dev. Dyn.* **238,** 632–640.

Mori, S., Itoh, R., Zhang, J., Kaufmann, W. E., van Zijl, P. C., Solaiyappan, M., and Yarowsky, P. (2001). Diffusion tensor imaging of the developing mouse brain. *Magn. Reson. Med.* **46,** 18–23.

Nieman, B. J., Flenniken, A. M., Adamson, S. L., Henkelman, R. M., and Sled, J. G. (2006). Anatomical phenotyping in the brain and skull of a mutant mouse by magnetic resonance imaging and computed tomography. *Physiol. Genomics* **24,** 154–162.

Nieman, B. J., Lerch, J. P., Bock, N. A., Chen, X. J., Sled, J. G., and Henkelman, R. M. (2007). Mouse behavioral mutants have neuroimaging abnormalities. *Hum. Brain Mapp.* **28,** 567–575.

Nieman, B. J., Szulc, K. U., and Turnbull, D. H. (2009). Three-dimensional, in vivo MRI with self-gating and image coregistration in the mouse. *Magn. Reson. Med.* **61,** 1148–1157.

Olsson, M., Campbell, K., and Turnbull, D. H. (1997). Specification of mouse telencephalic and mid-hindbrain progenitors following heterotopic ultrasound-guided embryonic transplantation. *Neuron* **19,** 761–772.

Parnell, S. E., O'Leary-Moore, S. K., Godin, E. A., Dehart, D. B., Johnson, B. W., Allan Johnson, G., Styner, M. A., and Sulik, K. K. (2009). Magnetic resonance microscopy defines ethanol-induced brain abnormalities in prenatal mice: Effects of acute insult on gestational day 8. *Alcohol. Clin. Exp. Res.* **33,** 1001–1011.

Petiet, A. E., Kaufman, M. H., Goddeeris, M. M., Brandenburg, J., Elmore, S. A., and Johnson, G. A. (2008). High-resolution magnetic resonance histology of the embryonic and neonatal mouse: A 4D atlas and morphologic database. *Proc. Natl. Acad. Sci. USA* **105,** 12331–12336.

Phoon, C. K., and Turnbull, D. H. (2003). Ultrasound biomicroscopy-Doppler in mouse cardiovascular development. *Physiol. Genomics* **14,** 3–15.

Phoon, C. K., Aristizabal, O., and Turnbull, D. H. (2000). 40 MHz Doppler characterization of umbilical and dorsal aortic blood flow in the early mouse embryo. *Ultrasound Med. Biol.* **26,** 1275–1283.

Phoon, C. K., Aristizabal, O., and Turnbull, D. H. (2002). Spatial velocity profile in mouse embryonic aorta and Doppler-derived volumetric flow: A preliminary model. *Am. J. Physiol. Heart Circ. Physiol.* **283,** H908–H916.

Phoon, C. K., Ji, R. P., Aristizabal, O., Worrad, D. M., Zhou, B., Baldwin, H. S., and Turnbull, D. H. (2004). Embryonic heart failure in NFATc1−/− mice: Novel mechanistic insights from in utero ultrasound biomicroscopy. *Circ. Res.* **95,** 92–99.

Punzo, C., and Cepko, C. L. (2008). Ultrasound-guided in utero injections allow studies of the development and function of the eye. *Dev. Dyn.* **237,** 1034–1042.

Schneider, J. E., Bamforth, S. D., Farthing, C. R., Clarke, K., Neubauer, S., and Bhattacharya, S. (2003a). Rapid identification and 3D reconstruction of complex cardiac malformations in transgenic mouse embryos using fast gradient echo sequence magnetic resonance imaging. *J. Mol. Cell. Cardiol.* **35,** 217–222.

Schneider, J. E., Bamforth, S. D., Grieve, S. M., Clarke, K., Bhattacharya, S., and Neubauer, S. (2003b). High-resolution, high-throughput magnetic resonance imaging of mouse embryonic anatomy using a fast gradient-echo sequence. *MAGMA* **16,** 43–51.

Schneider, J. E., Bose, J., Bamforth, S. D., Gruber, A. D., Broadbent, C., Clarke, K., Neubauer, S., Lengeling, A., and Bhattacharya, S. (2004). Identification of cardiac malformations in mice lacking Ptdsr using a novel high-throughput magnetic resonance imaging technique. *BMC Dev. Biol.* **4,** 16.

Sharpe, J., Ahlgren, U., Perry, P., Hill, B., Ross, A., Hecksher-Sorensen, J., Baldock, R., and Davidson, D. (2002). Optical projection tomography as a tool for 3D microscopy and gene expression studies. *Science* **296,** 541–545.

Shepherd, T. M., Thelwall, P. E., Stanisz, G. J., and Blackband, S. J. (2009). Aldehyde fixative solutions alter the water relaxation and diffusion properties of nervous tissue. *Magn. Reson. Med.* **62,** 26–34.

Smith, B. R. (2001). Magnetic resonance microscopy in cardiac development. *Microsc. Res. Tech.* **52,** 323–330.

Smith, B. R., Johnson, G. A., Groman, E. V., and Linney, E. (1994). Magnetic resonance microscopy of mouse embryos. *Proc. Natl. Acad. Sci. USA* **91,** 3530–3533.

Smith, B. R., Linney, E., Huff, D. S., and Johnson, G. A. (1996). Magnetic resonance microscopy of embryos. *Comput. Med. Imaging Graph.* **20,** 483–490.

Srinivasan, S., Baldwin, H. S., Aristizabal, O., Kwee, L., Labow, M., Artman, M., and Turnbull, D. H. (1998). Noninvasive, in utero imaging of mouse embryonic heart development with 40-MHz echocardiography. *Circulation* **98,** 912–918.

Sun, S. W., Neil, J. J., and Song, S. K. (2003). Relative indices of water diffusion anisotropy are equivalent in live and formalin-fixed mouse brains. *Magn. Reson. Med.* **50,** 743–748.

Sun, S. W., Liang, H. F., Xie, M., Oyoyo, U., and Lee, A. (2009). Fixation, not death, reduces sensitivity of DTI in detecting optic nerve damage. *Neuroimage* **44,** 611–619.

Turnbull, D. H., and Foster, F. S. (2002). In vivo ultrasound biomicroscopy in developmental biology. *Trends Biotechnol.* **20,** S29–S33.

Turnbull, D. H., and Mori, S. (2007). MRI in mouse developmental biology. *NMR Biomed.* **20,** 265–274.

Turnbull, D. H., Bloomfield, T. S., Baldwin, H. S., Foster, F. S., and Joyner, A. L. (1995). Ultrasound backscatter microscope analysis of early mouse embryonic brain development. *Proc. Natl. Acad. Sci. USA* **92,** 2239–2243.

Wadghiri, Y. Z., Blind, J. A., Duan, X., Moreno, C., Yu, X., Joyner, A. L., and Turnbull, D. H. (2004). Manganese-enhanced magnetic resonance imaging (MEMRI) of mouse brain development. *NMR Biomed.* **17,** 613–619.

Wadghiri, Y. Z., Schneider, A. E., Gray, E. N., Aristizabal, O., Berrios, C., Turnbull, D. H., and Gutstein, D. E. (2007). Contrast-enhanced MRI of right ventricular abnormalities in Cx43 mutant mouse embryos. *NMR Biomed.* **20,** 366–374.

Walls, J. R., Coultas, L., Rossant, J., and Henkelman, R. M. (2008). Three-dimensional analysis of vascular development in the mouse embryo. *PLoS ONE* **3,** e2853.

Weiner, H. L., Bakst, R., Hurlbert, M. S., Ruggiero, J., Ahn, E., Lee, W. S., Stephen, D., Zagzag, D., Joyner, A. L., and Turnbull, D. H. (2002). Induction of medulloblastomas in mice by sonic hedgehog, independent of Gli1. *Cancer Res.* **62,** 6385–6389.

Wichterle, H., Turnbull, D. H., Nery, S., Fishell, G., and Alvarez-Buylla, A. (2001). In utero fate mapping reveals distinct migratory pathways and fates of neurons born in the mammalian basal forebrain. *Development* **128,** 3759–3771.

Wiesmann, F., Ruff, J., Hiller, K. H., Rommel, E., Haase, A., and Neubauer, S. (2000). Developmental changes of cardiac function and mass assessed with MRI in neonatal, juvenile, and adult mice. *Am. J. Physiol. Heart Circ. Physiol.* **278,** H652–H657.

Zhang, J., Richards, L. J., Yarowsky, P., Huang, H., van Zijl, P. C., and Mori, S. (2003). Three-dimensional anatomical characterization of the developing mouse brain by diffusion tensor microimaging. *Neuroimage* **20,** 1639–1648.

Zhang, J., Chen, Y. B., Hardwick, J. M., Miller, M. I., Plachez, C., Richards, L. J., Yarowsky, P., van Zijl, P., and Mori, S. (2005a). Magnetic resonance diffusion tensor microimaging reveals a role for Bcl-x in brain development and homeostasis. *J. Neurosci.* **25,** 1881–1888.

Zhang, J., Miller, M. I., Plachez, C., Richards, L. J., Yarowsky, P., van Zijl, P., and Mori, S. (2005b). Mapping postnatal mouse brain development with diffusion tensor microimaging. *Neuroimage* **26,** 1042–1051.

Zhou, Y. Q., Foster, F. S., Qu, D. W., Zhang, M., Harasiewicz, K. A., and Adamson, S. L. (2002). Applications for multifrequency ultrasound biomicroscopy in mice from implantation to adulthood. *Physiol. Genomics* **10,** 113–126.

Zhou, Y. Q., Foster, F. S., Parkes, R., and Adamson, S. L. (2003). Developmental changes in left and right ventricular diastolic filling patterns in mice. *Am. J. Physiol. Heart Circ. Physiol.* **285,** H1563–H1575.